

Hot side flow investigation on the exhaust case of a recuperated industrial gas turbine

Stefan Ahlinder¹, Volker Biesold², Heinz Peter Berg²

¹ Vattenfall (KKW Forsmark), Bereich Strömungsmechanik

² Lehrstuhl Verbrennungskraftmaschinen und Flugantriebe

Kurzfassung

Das Strömungsfeld der Abgaseinheit einer kompakten Industriegasturbine wurde experimentell, wie auch numerisch untersucht. Für die experimentellen Untersuchungen wurde ein Plexiglasmodell mit einem originalen Wärmetauscher an einem Wasseranalogiekanal adaptiert. In den numerischen Berechnungen wurde der Wärmetauscher (HEX) als poröses Medium modelliert. Für den vorliegenden Fall fand der Code eines Porositätsmodells Verwendung, der am Lehrstuhl Verbrennungskraftmaschinen und Flugantriebe im Rahmen des Aerohex Projektes [1] entwickelt wurde. Das Ziel der durchgeführten CFD Berechnungen ist es, herauszufinden ob der Einfluss des HEX auf das Strömungsfeld numerisch nachgewiesen werden kann, wenn der Wärmetauscher als poröses Medium behandelt wird. In den Untersuchungen wurden der Einströmwinkel, die Reynolds Zahl und die Geometrie des Modells variiert. Es hat sich experimentell wie auch in den numerischen Betrachtungen gezeigt, dass der Einfluss des Einströmwinkels auf das Strömungsfeld vernachlässigbar ist, so wie die Reynolds-Zahl auf die untersuchten Volumenströme. Die Geometrie stromauf des HEX hat somit nur einen geringen Einfluss auf das Strömungsfeld. Die im Experiment beobachteten Hauptströmungsstrukturen finden sich auch in den numerischen Ergebnissen wieder. Das in der Numerik generierte Strömungsfeld stimmt so gut mit den Experimenten überein, dass man das CFD Tool mit Sicherheit für zukünftige Designstudien verwenden kann.

Abstract

The flow field of the exhaust gas casing of a compact industrial gas turbine has been investigated experimentally as well as numerically. For the experimental investigations a Perspex model with a real heat exchanger mounted inside was used in a water analogy test facility. In the numerical calculations the heat exchanger (HEX) was modelled as a porous medium. For this purpose a porosity model code, that has been developed at the Chair of Combustion Engines and Flight Propulsion (LS VFA) at BTU within the Aerohex project [1], was used. The purpose of performing CFD calculations is to find out if the influence of the HEX on the flow field can be achieved numerically by treating the heat exchanger as a porous medium. During the investigations the inflow angle, the Reynolds number and the geometry were varied. It was shown both experimentally and numerically that the influence from the inlet flow angle on the flow field was negligible, as was the Reynolds number for the range of flows

investigated. The geometry up stream of the HEX had also a minor influence on the flow field. The major flow structures that were observed experimentally were also seen in the numerical results. The flow field produced by the CFD code agrees well with the experimental and indicates that the CFD tool can be used with confidence for future design studies.

Introduction

It is of large interest to increase the efficiency and thereby reduce fuel consumption and CO₂ emissions for gas turbines. One method to do this is to increase the turbine inlet temperature. This is a track that has been followed over many years leading to higher and higher turbine temperature loads. Without major improvements in turbine material technology the possibilities for further temperature rises are limited. A different way of improving fuel economy would be to use a recuperator to make use of the heat of the exhaust gases that otherwise is lost. This is the concept of the compact industrial gas turbine that has been investigated. The aim of the task was to investigate the flow field around the exhaust gas heat exchanger in a compact gas turbine, experimentally as well as numerically.

Experimental part

The water analogy test facility of the Chair VFA was used for the flow investigations of the exhaust gas casing of a typical industrial recuperated gas turbine. The point in using a water channel, for such investigations, is that for the same Reynolds number as in a real machine, with gas as working medium, the flow velocities are significantly lower which enables better possibilities for flow visualisations.

During the design of the test model the following criteria were given:

- it should be possible to adjust the distance between diffusor and HEX
- it should be possible to adjust the horizontal position of the HEX
- the model should be made of Perspex
- it should be possible to adjust the inlet swirl, between -20 and +20 degrees
- the mass flow rates should, if possible, correspond to between 25 % till over 100 % load

Water analogy test facility

The water channel (wc) is suitable for investigations of incompressible flow where the laws of analogy, in this case Reynolds number, can be applied. For the investigations a Perspex model of an exhaust gas exit casing was constructed and mounted to the water channel. The facility itself, see fig. 1 below, has a 2.7 m high platform which measures 5,2 x 7,4 m with a desk from which the water channel is controlled. Below the platform are the water reservoir and the pump equipment located. Underneath the experimental model there is a plenum chamber where pressurized air can be supplied for visualisation purposes. In order to avoid suction effects on the experimental model the water is led through a tube to the back flow serpentine where the water is vented and reaches atmospheric pressure. The operating condition, i.e. the water flow, is set by using an inductive flow meter.

Water analogy test facility technical data:

Volume flow: 180 l/s	Water in circulation: 2 m ³
Control range: 25-180 l/s	Water reservoir: 22,3 m ³
Maximum pump head: 27 m	Pump power: 70 kW

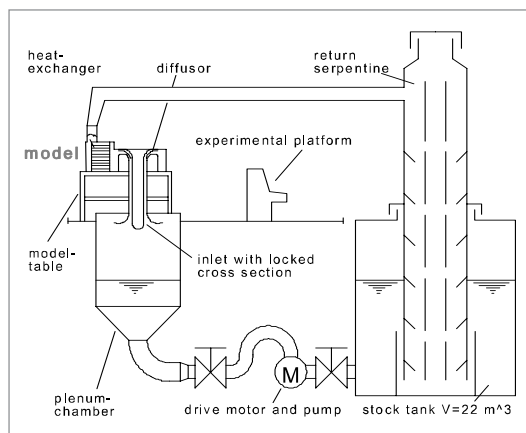


Figure 1:
Water analogy test facility.

Experimental model

The model was built of Perspex as a 1:1 scale model of an exhaust gas casing of a typical compact industrial gas turbine. In order to meet the set up demands it was decided to choose two configurations, see fig. 2. The two configurations cover, to some extent, the demands put on the model regarding variable distance between diffuser and HEX and horizontal position of the HEX.

At the model inlet and outlet the total and the static pressures were measured, the different measurement positions are shown in fig. 3. At the model inlet static pressure was measured at six azimuthally equidistant positions. For the total pressure measurements six multi-function measurement flanges were mounted at the same azimuthal positions as the static measurement positions. At these flanges a traversable total pressure probe was mounted, which made it possible to traverse over the whole radius and to measure the total pressure profiles at six different positions.

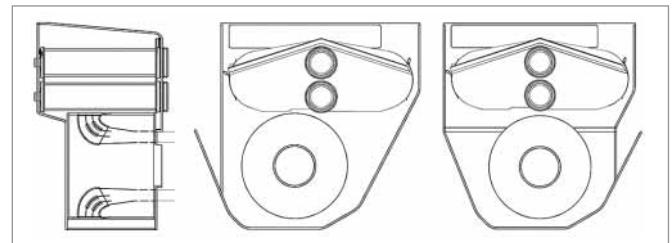


Figure 2:
Side and front views of the Perspex model for configuration 1 and 2.

At the model exit 20 positions – 10 on each side of the outlet, were drilled for static measurements. The total pressure was measured by traversing 16 total pressure probes, shown also in fig. 3. All pressures were measured as difference pressure with the plenum chamber pressure as reference pressure.

To realize inlet swirl angles between -20 and +20 degrees 20 guide vanes were mounted upstream of the model inlet. The guide vanes were mounted from outside the outer tube of the inlet part of the model.

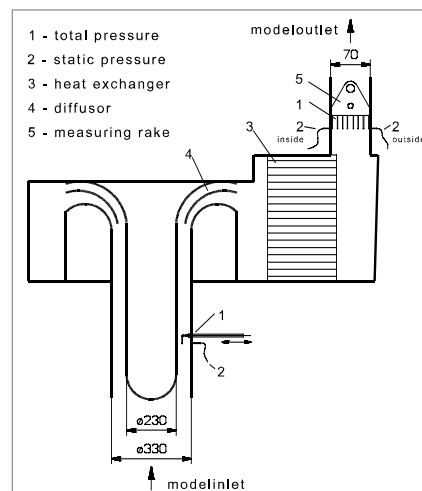


Figure 3:
Measurement positions on the experimental model.

In order to have optimal conditions for visualization of the flow the model was made of Perspex. The experimental model itself could not be built strong enough to withstand the loads that arise in the water channel. Therefore a stronger outer Perspex casing was constructed to take the load. When designing a transparent model for visualizations, care has to be taken regarding the refraction problems that occur from the refraction of the path of rays at the boundary surfaces between the different materials. In order to reduce these problems the model itself was constructed of 5 mm thin Perspex walls and the load carrying outer casing of the model was constructed with thick plane Perspex walls formed as a polygon with six flat walls, see fig. 4. By using an outer casing, flat side walls could be used in order to reduce refraction problems. For security reasons reinforcements, in the form of beams on top and along the sides of the model were mounted, see fig. 4.

In order to achieve the correct influence of the heat exchanger on the flow field a real heat exchanger was used instead of just device giving a certain flow resistance.

For the visualizations it was necessary that the model of the exhaust gas casing was easy to overlook. The model of the exhaust gas casing was manufactured completely of perspex except for the heat exchanger, which was an original part, and the connections to the water channel, which were made of metal.

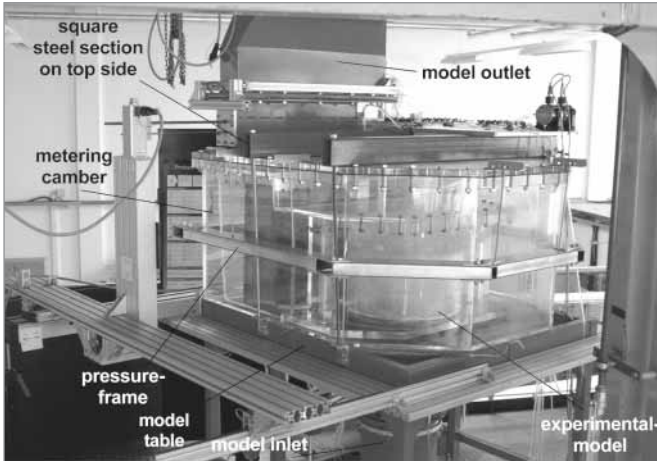


Figure 4:
Water analogy test facility with the experimental model

Operational conditions

The operational conditions, corresponding to 100 % load, for the industrial gas turbine, were supplied by MTU [2].

HEX casing inlet total pressure: 1,0763 Bar
 Total pressure upstream of the HEX: 1,015 Bar
 Total pressure downstream of the HEX: 0,974 Bar
 Gas mass flow: 2,92 kg/s
 HEX casing inlet gas temperature: 1039 K

In order to keep the Re number the same in the water channel as in the operational condition above the corresponding water mass flow has to be determined. This is done by using the following well known relations:

$$Re_{\text{water}} = Re_{\text{gas}}, \text{ expressed as: } \frac{U_{\text{water}} \cdot D}{\nu_{\text{water}}} = \frac{U_{\text{gas}} \cdot D}{\nu_{\text{gas}}}$$

A combination of the equation above and the mass conservation equation leads to:

$$\frac{\dot{m}_{\text{water}} \cdot D}{\rho_{\text{water}} \cdot A \cdot \nu_{\text{water}}} = \frac{\dot{m}_{\text{gas}} \cdot D}{\rho_{\text{gas}} \cdot A \cdot \nu_{\text{gas}}}$$

from which the water mass flow can be deduced as the product of the gas flow and the ratio of dynamic viscosities:

$$\dot{m}_{\text{water}} = \dot{m}_{\text{gas}} \cdot \frac{\mu_{\text{water}}}{\mu_{\text{gas}}}$$

$$\mu_{\text{water}} = 8,57 \cdot 10^{-4} \text{ [Pa.s]}, \text{ corresponding to } 300 \text{ K,}$$

$$\mu_{\text{gas}} = 4,45 \cdot 10^{-5} \text{ [Pa.s]}, \text{ corresponding to } 1039 \text{ K}$$

From the viscosities and the equation above the water mass flow is calculated to:

$$\dot{m}_{\text{water}} = 56,2 \text{ [kg/s]} \text{ (corresponding to } 100 \% \text{ load)}$$

It was decided to choose the inlet flow angles -20, -10, 0, +10 and +20 degrees for the investigations.

Measurement equipment

At the model entrance the static pressure was measured at six locations. For the measurement of the total pressure a traversable probe was used. The probe, mounted at the multi-function measurement flange, could be traversed in the radial direction. The arrangement of the flanges made it possible to measure six total pressure profiles distributed over the inlet.

At the model outlet there are 20 positions for the static pressure on the two long sides of the outlet, ten on each. For the measurement of the total pressure at the model outlet a measuring rake was used. The rake carries 16 pressure measuring tubes. The tubes seize the total pressure at fixed positions on the width of the outlet cross-section. The measuring rake is led by two tubes and can be traversed over the length of the outlet cross-section. This made it possible to measure the outlet total pressure field.

At the model inlet seven (1+6) pressure measurement locations were used. At the model outlet 36 (16+10+10) pressure measurement locations were used.

A system of wet/wet difference pressure transducers of type Sensotec model Z with the ranges 0-35 mbar and 0-100 mbar were used for the pressure difference measurements. The measuring amplifier, of type DMCplus by HBM, was applied and the data acquisition was made completely on a PC with the control software LabVIEW.

Methods of visualization

At the LS VFA there are different methods available for flow visualization, e.g. PIV, LDA, air bubbles and dye. Due to the geometrical configuration of the experimental model PIV and LDA were unsuitable. Instead air bubbles were injected in order to get an impression of the major flow characteristics. The bubbles follow the flow and can be observed and photographed. The air injection system consists of 6 tubes of porous sinter metal that are located around the circumferential in the lower part of the plenum chamber. The air bubbles can be observed using day-light or if a laser light cut is done a two-dimensional observation is possible. The bubbles within the light cut reflect the light and stand then out clearly against the background. Over the long-term exposure of a photo camera the course of the air bubbles can be captured and documented. Results are so-called streak-line picture recordings. The streak-lines show the movements of the fluid. Apart from the streak-line picture recordings the

air bubble method can be used together with video recordings. In this way the long-term behaviour can be examined. The air bubble method supplies high-quality reproducible flow patterns and makes a descriptive documentation possible. To avoid buoyancy effects it is necessary to keep the bubble size as small as possible. Additionally, it helps to run the experiments at a relatively high flow rate. When visualizing the flow, the flow rates were usually in the range of 83,17-88,16 kg/s. For comparative reasons a couple of tests were made with flow rates around 49,9 kg/s.

For the visualization an argon ion laser system, 543 Series, model 543-MB-A01 was used. For documentation a CCD S/W camera was used. For long-term photographs a digital video camera was used. The observation of the eddy structures in the top of the front of the heat exchanger took place in this way. The best results during the visualization of the flow structures were achieved with photographs of so-called streak-lines. For all interesting ranges and flow features a set of photographs were made.

A further possibility for flow visualization is the use of threads. The thread aligns itself along the flow and indicates also by the intensity of the "flutter" turbulence areas. Threads were used at the inner and outer wall of the model inlet, upstream of the diffuser in order to see the swirl effect of the inlet guide vanes.

Numerical part

For the numerical investigations the commercial CFD-code CFX-TASCflow, version 2.12.0-521 [4], was used in combination with the porosity model code developed at LS VFA at BTU. CFX-TASCflow is a multi purpose CFD software with a coupled multigrid solver that works on block structured hexa meshes. The software offers the possibility to add sources to the transport equations making it possible to e.g. simulate the influence of a heat exchanger in a computational domain. The porosity model code, which adds sink terms to the momentum equations, has been linked to the CFX-TASCflow solver and been used for the calculations.

The calculations were performed in parallel on a 2 processor PC with 2 AMD Athlon 2.4 GHz processors with a convergence criterion of $1E-4$ for the maximum residuals of the continuity equation.

As previously mentioned two different geometrical configurations were to be investigated. This also means that two different geometries had to be meshed, for instance see fig. 5 below. The meshing was made by using the commercial software ICEM-CFD, version 4.2. Due to the memory limitations of the 32 bit version of TASCflow the grid size was restricted to be not larger than 1,8-1,9 million nodes. Configuration 1 that was more complicated to mesh, and that required more nodes than configuration 2, has a mesh consisting of about 1,83 million nodes. In order to make the results from the two different configurations comparable the mesh resolutions were tried to be kept the same. This led to a slightly smaller mesh for configuration 2, consisting of around 1,5 million nodes. In fig. 5 the entire geometry is shown to give just an overview of the meshes and the geometries. In fig. 6 the mesh for the HEX, which is identical for both configurations, is shown.

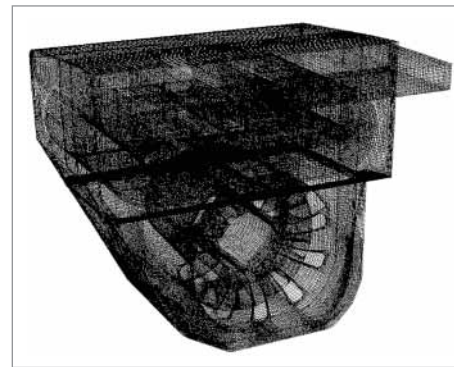


Figure 5:
Configuration 1 mesh.

As described in chapter "operational conditions", it was decided to study the flow field for five different inlet angles (-20, -10, 0, +10 and +20 degrees). Furthermore, it was also decided to investigate the influence of the Reynolds number and to let them vary between around 25 % till over 100 % of full load. For the calculations the mass flows 19, 40, 60 and 83 kg/s, which correspond do between 34 % and 148 % of full load, were chosen.

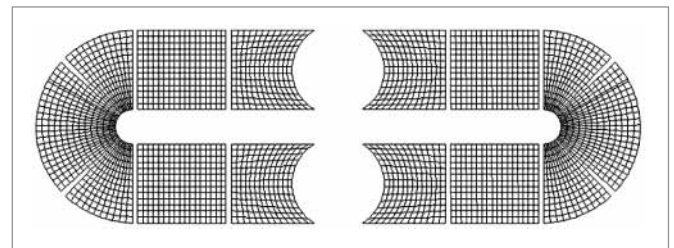


Figure 6:
Mesh of the HEX, side view.

Three different boundary conditions have been used, inlet, wall and outlet. Since the flow is considered isothermal and incompressible there are no pressure or temperature depending fluid quantities involved, making it possible to leave the energy equation out. The pressure level can be chosen arbitrarily, and in order to reduce the numerical error that could arise from large pressure values, the outlet average static pressure was set to zero. The boundary conditions used are summarized below.

- Inlet: mass flow and direction vector, turbulent intensity of 0,1 and turbulent length scale of 0,01 m.
- Outlet: outlet, average static pressure set equal to zero.
- Wall: No slip condition, and the fixed wall distance wall function used.

The relatively coarse mesh that was used, due to memory limitations, made it meaningless to apply a higher order numerical scheme for the calculations. Instead, a first order upwind scheme, which is known to be very robust, although diffusive and less accurate, was used for the advection terms. Another problem, caused by the coarse mesh, is that the boundary layers can not be calculated satisfactorily. When the mesh is relatively coarse, it is only possible to use wall functions, i.e. model the viscous sub-layer. When using the standard wall function formulation, there are certain limitations on the near wall mesh size in order to calculate a reasonable wall shear stress. In order to reduce these

uncertainties the fixed wall distance wall function by Grotjans and Menter [4] was used. The main numerical settings are in summary:

1. Flow considered incompressible and steady.
2. Water properties corresponding to 300 K with a density of 997 kg/m^3 and a dynamic viscosity of $8,57 \cdot 10^{-4} \text{ Ns/m}^2$
3. A convergence criterion of $1E-4$ was used for the maximum residuals for the continuity equation.
4. The porosity model resistance tensors used are the same as described in the porosity model report [1].
5. Standard k-epsilon turbulence model with the fixed wall distance wall function.
6. First order upwind scheme for the advection terms.

Results

Pressure drops, velocity profiles at inlet and outlet have been measured and the flow field has been visualized in the casing below the HEX and at HEX outlet. During the measurement campaigns the following parameters have been varied:

1. Inlet flow angle
2. Reynolds number
3. Geometry (2 different configurations)

The turbulent intensity was measured by the use of a hot-wire for water applications for two different Reynolds numbers. When using the hot-wire in water the temperature difference between wire and water must not be too large in order to avoid generation of bubbles. Therefore the uncertainties for measurements in water are larger than in air where a higher wire temperature can be used. The measured turbulent intensity was for a Reynolds number of $1,06E5$ about 12 % and for a Reynolds number of $1,47E5$ about 10 %.

Inlet velocity profiles

The inlet velocity profiles were derived from the measured static and total pressures at the inlet plane. The inlet geometry had to be adjusted and the angle of the guide vanes had to be adjusted very carefully in order to get symmetric flow conditions. In fig. 7 below the inlet velocity profiles are shown for different Reynolds numbers. The figure shows the independence of the Reynolds number if the Reynolds number is high enough. For flows in the model lower than 2500 l/min the flow could not be maintained steady enough to ensure reliable measurements. This is obvious from fig. 7 where the profile for the lowest Reynolds number differs significantly from the others. In fig. 8 profiles for different inlet angles are presented, showing no significant difference between the profiles for the different inflow angles. In fig. 9 it is shown that the measurement positions are placed far enough down stream of the inlet guide vanes in order to have the influence of the guide vanes on the velocity profiles lost. The velocity profiles for three neighbouring measurement flanges are very close to each other.

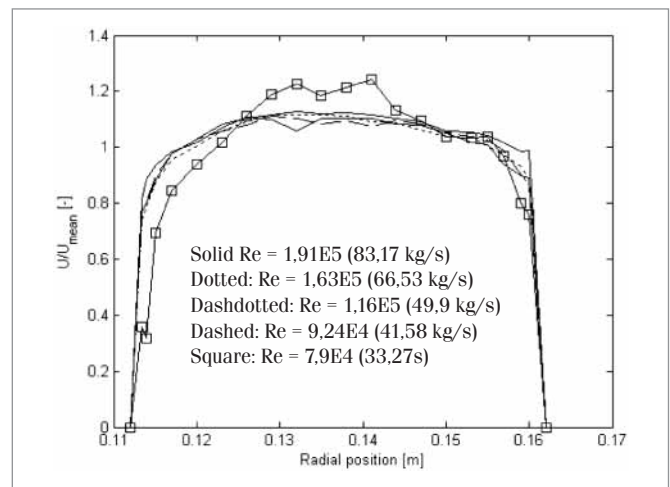


Figure 7:
Inlet velocity profiles for different Reynolds number. Inlet flow angle of 20 deg.

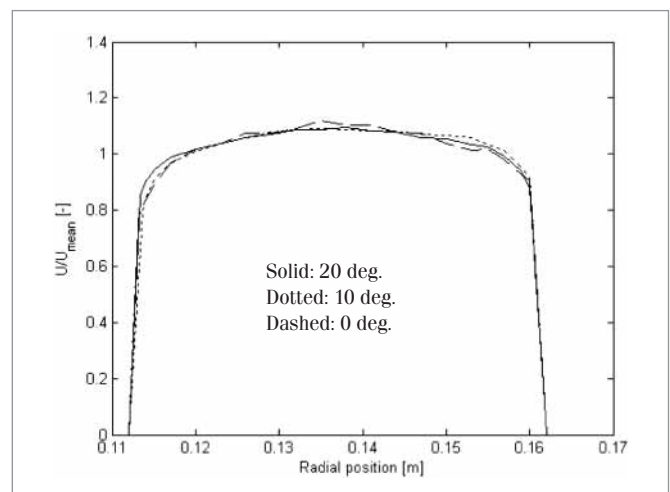


Figure 8:
Inlet velocity profiles for different inlet flow angles.

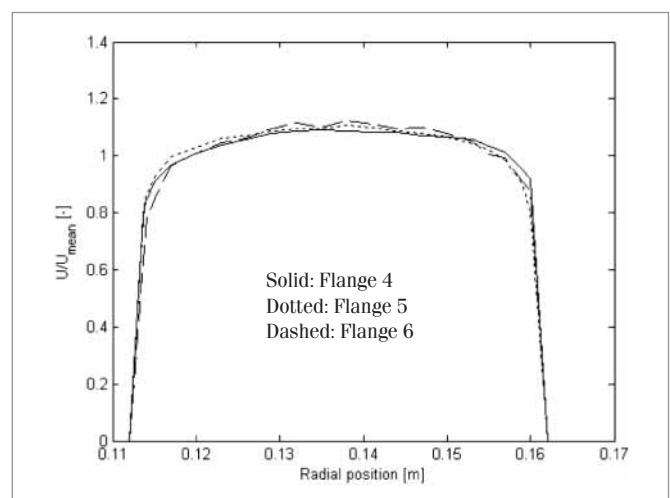


Figure 9:
Inlet velocity profiles for different azimuthal positions.

Outlet pressure field

To make the measured and calculated outlet pressure fields comparable a non-dimensional pressure coefficient has been used. The pressure coefficient is defined as:

$$P^* = \frac{P_{total} - P_{total, min}}{P_{dynamic, inlet}}$$

Below, as an example, the pressure coefficient has been plotted for one of the cases studied. As can be noticed in the fig. 10 below the variation in the total pressure field is larger in the experimental results than in the numerical ones. However, the main pressure field characteristics, the separation zone at the top and the region of high pressure at the right part of the exhaust duct, are captured by the numerical simulation.

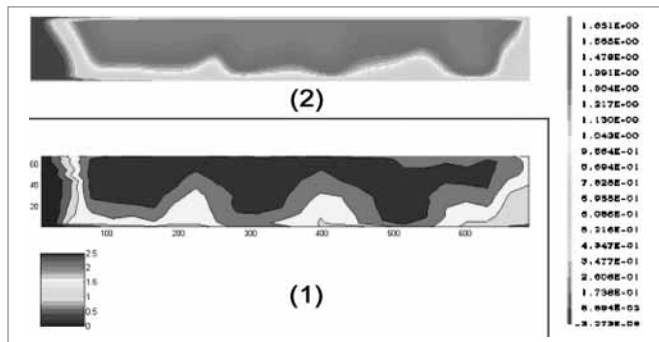


Figure 10: Measured (1) and calculated (2) pressure coefficient for configuration 1.

Flow field visualizations

Note: The Perspex model and the numerical model were, by mistake, mirrored compared to each other. This does not make the results incomparable, but should be considered when studying the results in the figures below.

The inlet flow angle has a negligible influence on the flow field due to the straightening of the flow that takes place between the diffuser struts. This was clearly seen in the experiments and was visualized with air. The same straightening effect of the flow was seen in the numerical results. This is illustrated in the vector plot in fig. 11.

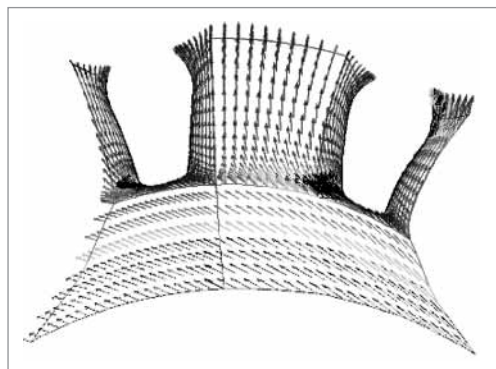


Figure 11: Flow straightening effect between the struts in the CFD results, 20 deg inlet angle.

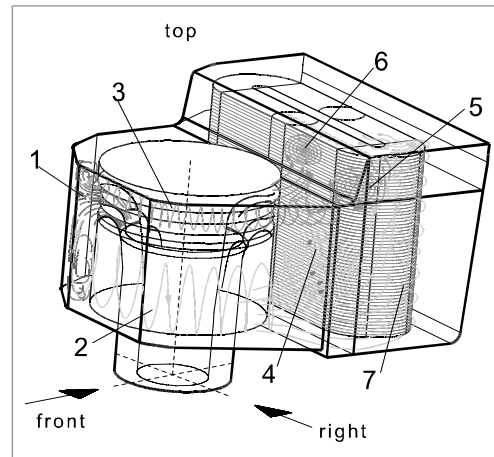


Figure 12: Flow characteristics in the exhaust gas casing.

The flow field in the casing below the heat exchanger, for both configurations, is characterized by the vortices generated at each side of the diffuser outlet and directed towards the HEX, see vortices 2 and 3 in fig. 12. Furthermore, there are vortices generated downstream of the diffuser just below the HEX from the flow coming out of the diffuser, vortex 6 in fig. 12. These flow features are seen both in the experiments and in the numerical results and are shown in the picture below, fig. 12, where the main flow structures are sketched. Examples of the corresponding experimental and numerical pictures are presented directly after with the different vortex positions in fig. 12 numbered.



Figure 13: Vortices created at the diffuser outlet, configuration 1, positions 2 and 3.

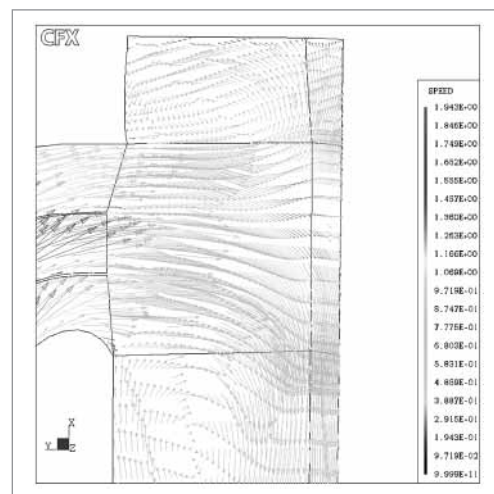


Figure 14: Calculated vortices at the diffuser outlet, configuration 1, positions 2 and 3.

Stefan Ahlinder¹, Volker Biesold², Heinz Peter Berg²

¹ Vattenfall (KKW Forsmark), Bereich Strömungsmechanik

² Lehrstuhl Verbrennungskraftmaschinen und Flugantriebe



Figure 15:
Flow field at the side below the HEX, configuration 2, position 5.

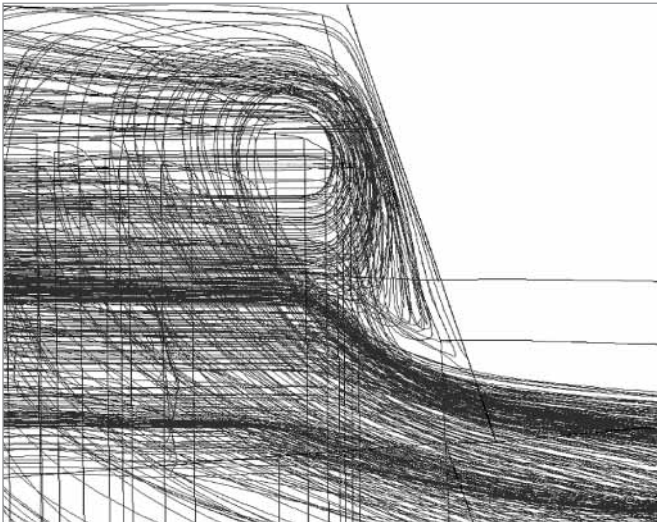


Figure 16:
Calculated flow field at the side below the HEX, configuration 2, position 5.



Figure 17:
Flow field below the HEX, configuration 2, position 4.

The flow field downstream of the HEX is characterized by the relatively high velocities in the bend regions giving rise to vortices directed towards the exhaust duct. This is also seen in the numerical results, although the vortices are not as strong as in the experimental visualizations. As can be seen in the following pictures the large scales of the flow field are similar in the experimental and the numerical results, and also between the two configurations. Due to the fact that the bend covers leave an area around the bend spacers open for flow, quite high velocities are noticed in these regions. This is clearly seen in the experimental visualizations, as well as in the numerical results, see figures below. The numerical results indicate a higher flow rate through the HEX in the region closest to the exhaust duct. This trend can also be noticed in the flow results, see fig. 18, but is not as clear as in the numerical results.

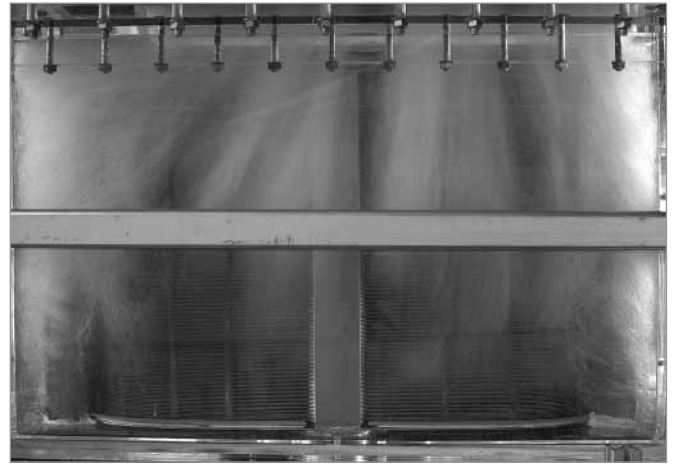


Figure 18:
HEX outlet flow field, configuration 2.

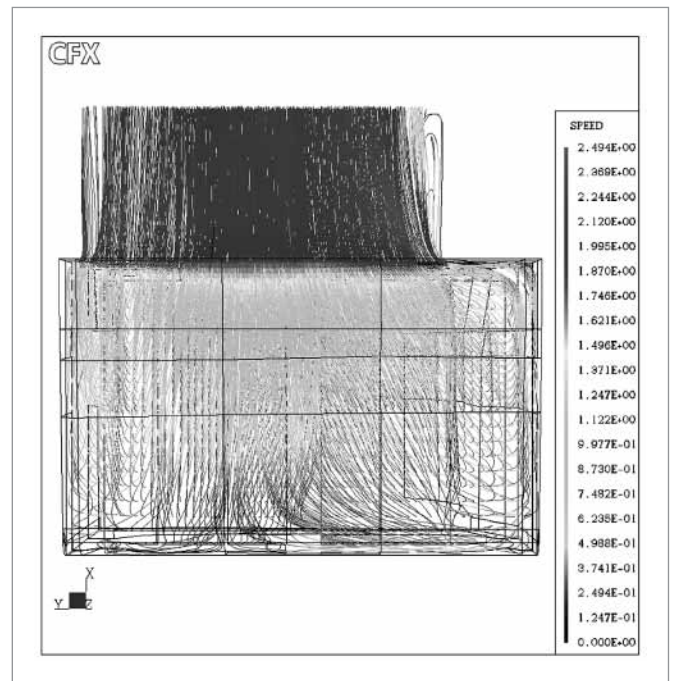


Figure 19:
Calculated HEX outlet flow field, configuration 2.

Stefan Ahlinder¹, Volker Biesold², Heinz Peter Berg²¹ Vattenfall (KKW Forsmark), Bereich Strömungsmechanik² Lehrstuhl Verbrennungskraftmaschinen und Flugantriebe

Conclusions

Investigations, experimental and numerical, have been undertaken on a Perspex model of a typical compact industrial gas turbine. During the investigations the inflow angle, the Reynolds number and the geometry were varied. It was shown both experimentally and numerically that the influence from the inlet flow angle on the flow field was negligible, as was the Reynolds number for the range of flows investigated. The geometry up stream of the HEX had also a minor influence on the flow field.

The major flow structures that were observed experimentally were also seen in the numerical results and, although no real validation of the CFD code could be made, regarding pressure drop, the flow field produced by the CFD code agrees well enough with the experiments in order to be safe in using the CFD tool for future design studies.

A recommendation could be to try to cover the bends so that at least the bend spacers are covered. In the investigated configurations the flow through the bends is significantly much higher than through the straight parts, leading to an unnecessary efficiency reduction.

References

- [1] EU GROWTH PROJECT GRD1-1999-10602 "AEROHEX": Deliverable 7, Report on the Derivation of the Porosity Model.
- [2] KATHEDER, K.: MTU Aero Engines, private communication
- [3] VDI WÄRMEATLAS: 9. Auflage, Springer 2002.
- [4] CFX-TASCFLOW: User Documentation, Version 2.11, June 2001, AEA Technology.
- [5] DR. REILE, E.: MTU Aero Engines, private communication



Dr.-Ing. Stefan Ahlinder wurde am 19. April 1967 in Uppsala/Schweden geboren. Er studierte von August 1989 bis Dezember 1993 an der Königlich Technischen Hochschule Stockholm (KTH) in der Fachrichtung Kraft- und Wärmetechnik. Nach dem Studium arbeitete er von Dezember 1993 bis September 1994 als Wissenschaftlicher Assistent am Lehrstuhl für Kraft- und Wärmetechnik der KTH Stockholm. Ab September 1994 erfolgte sein Einstieg als Trainee beim Energiekonzern Vattenfall Kernkraftwerk Forsmark/Schweden zum Berechnungsingenieur im Bereich Strömungs- und Wärmetechnik. Von September 2001 bis November 2004 promovierte er zum Thema „On Modelling of Compact Tube Bundle Heat Exchangers as Porous Media for Gas Turbine Engine Applications“ am Lehrstuhl Verbrennungskraftmaschinen und Flugantriebe der BTU Cottbus in Zusammenarbeit mit MTU München im Rahmen des AEROHEX-Programmes. Promotion im April 2006. Seit November 2004 ist er bei der Firma Vattenfall (KKW Forsmark) als Fachgebietsspezialist im Bereich Strömungsmechanik tätig.



Dipl.-Ing. Volker Biesold wurde am 13. Juni 1971 in Hoyerswerda geboren. Er studierte von September 1992 bis Januar 2002 an der BTU Cottbus in der Fachrichtung Allgemeiner Maschinenbau. Im Rahmen seiner Studienarbeit untersuchte er die Wirbelstrukturen in dem Modell einer neuartigen Zyklidbrennkammer. In seiner Diplomarbeit forschte er auf dem Gebiet der Filmkühlung und Strömungsablösung im Bereich moderner Hochleistungsturbinenschaufeln. Im Zuge seiner studentischen Mitarbeitertätigkeiten an den Lehrstühlen Konstruktion & Fertigung, Kraftwerkstechnik und Verbrennungskraftmaschinen & Flugantriebe sammelte er umfangreiche Erfahrungen auf dem Gebiet der Konstruktion von Versuchsmaschinen und der Messtechnik. So befasste er sich im Bereich der Strömungsmesstechnik u. a. eingehend mit der Hitzdrahtanemometry und der Laser Particle Image Velocimetry. Seit Februar 2002 ist er wissenschaftlicher Mitarbeiter am Lehrstuhl Verbrennungskraftmaschinen & Flugantriebe. Im Rahmen des AEROHEX-Programmes unterstützte er den Aufbau des Modellprüfstandes und führte die experimentellen Untersuchungen durch.



Prof. Dr.-Ing. Heinz Peter Berg wurde am 1. September 1960 in Friedberg/Hessen geboren. Er studierte von 1979 bis 1985 an der TH Darmstadt in der Fachrichtung Allgemeiner Maschinenbau. Nach dem Studium promovierte er am Fachgebiet Flugantriebe und Gasturbinen der TH Darmstadt. 1991 wechselte er zur neu gegründeten Triebwerksfirma BMW Rolls-Royce Aero Engines GmbH, die er mit aufbaute. Hier war er zunächst als Referent Prüfstandsentwicklung für die Auslegung und den Entwurf von neuen thermodynamischen sowie strömungstechnischen Testaufbauten, Komponenten- und Triebwerksprüfstände zuständig. 1992 übernahm er die Testprogrammleitung im F&E-Bereich der BMW Rolls-Royce Aero Engines GmbH. Anfang 1994 wurde er zum Leiter des aero-/thermodynamischen Komponentenversuchs (Strömungskomponenten- und Brennkammerversuch) ernannt. Ab 1994 übernahm er die Gesamtleitung der Abteilung Triebwerkskomponentenerprobung, bestehend aus den Fachgruppen Anbaugeräteerprobung und Triebwerksregelung; mechanische Bauteilerprobung; aero- und thermodynamischer Komponentenversuch. In dieser Zeit wurde das erste deutsche Ziviltriebwerk (BR 710) konzipiert, erprobt und für den Flugbetrieb zugelassen. 1995 erhielt er den Ruf an die BTU Cottbus. Seit Ende 1996 leitet er den Lehrstuhl Verbrennungskraftmaschinen und Flugantriebe mit den Forschungsgebieten Verbrennungsmotoren und Gasturbinen.